Effect of NiO inserted layer on spin-Hall magnetoresistance in Pt/NiO/YIG heterostructures

T. Shang, Q. F. Zhan, H. L. Yang, Z. H. Zuo, Y. L. Xie, L. P. Liu, S. L. Zhang, Y. Zhang, H. H. Li, B. M. Wang, Y. H. Wu, S. Zhang, and Run-Wei Li

---

Articles you may be interested in

Effect of IrMn inserted layer on anomalous-Hall resistance and spin-Hall magnetoresistance in Pt/IrMn/YIG heterostructures
J. Appl. Phys. **120**, 133901 (2016); 10.1063/1.4964114

Isothermal tuning of magnetic coercivity in NiFe/NiO/[Co/Pt] heterostructures with orthogonal easy axes
J. Appl. Phys. **118**, 093901 (2015); 10.1063/1.4929760

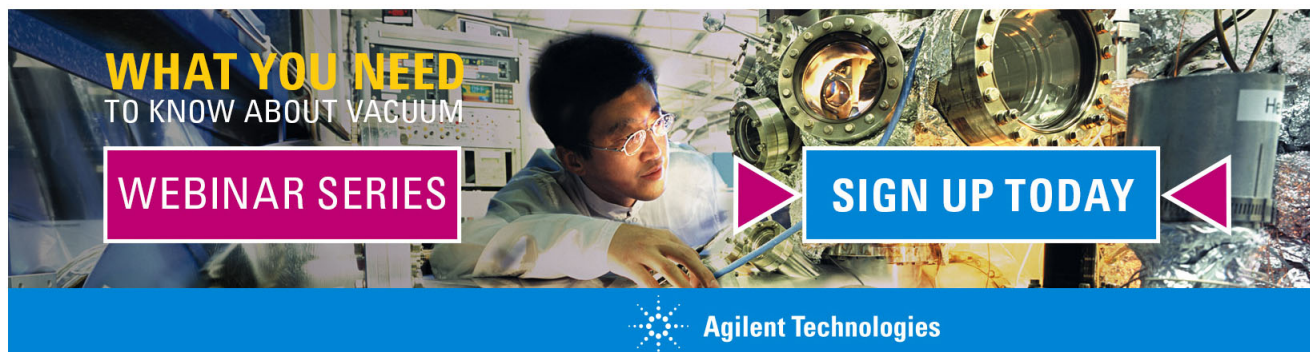Anti-damping spin transfer torque through epitaxial nickel oxide
Appl. Phys. Lett. **106**, 162406 (2015); 10.1063/1.4918990

Exchange magnetic field torques in YIG/Pt bilayers observed by the spin-Hall magnetoresistance
Appl. Phys. Lett. **103**, 032401 (2013); 10.1063/1.4813760

Polarity of anomalous Hall effect hysteresis loops in [Pt ∕ Co] 15 ∕ AF ∕ [Co ∕ Pt] 15 (AF = Fe Mn , NiO) multilayers with perpendicular anisotropy
J. Appl. Phys. **97**, 013901 (2005); 10.1063/1.1825628

Effect of NiO inserted layer on spin-Hall magnetoresistance in Pt/NiO/YIG heterostructures

T. Shang,[1,a)] Q. F. Zhan,[1,b)] H. L. Yang,[1] Z. H. Zuo,[1] Y. L. Xie,[1] L. P. Liu,[1] S. L. Zhang,[1] Y. Zhang,[1] H. H. Li,[1] B. M. Wang,[1] Y. H. Wu,[2] S. Zhang,[3,c)] and Run-Wei Li[1,d)]

[1]*Key Laboratory of Magnetic Materials and Devices and Zhejiang Province Key Laboratory of Magnetic Materials and Application Technology, Ningbo Institute of Material Technology and Engineering, Chinese Academy of Sciences, Ningbo, Zhejiang 315201, China*
[2]*Department of Electrical and Computer Engineering, National University of Singapore, 4 Engineering Drive 3, Singapore 117583*
[3]*Department of Physics, University of Arizona, Tucson, Arizona 85721, USA*

We investigate spin-current transport with an antiferromagnetic insulator NiO thin layer by means of the spin-Hall magnetoresistance (SMR) over a wide range of temperature in Pt/NiO/$Y_3Fe_5O_{12}$ (Pt/NiO/YIG) heterostructures. The SMR signal is comparable to that without the NiO layer as long as the temperature is near or above the blocking temperature of the NiO, indicating that the magnetic fluctuation of the insulating NiO is essential for transmitting the spin current from the Pt to YIG layer. On the other hand, the SMR signal becomes negligibly small at low temperature, and both conventional anisotropic magnetoresistance and the anomalous Hall resistance are extremely small at any temperature, implying that the insertion of the NiO has completely suppressed the Pt magnetization induced by the YIG magnetic proximity effect (MPE). The dual roles of the thin NiO layer are, to suppress the magnetic interaction or MPE between Pt and YIG, and to maintain efficient spin current transmission at high temperature. *Published by AIP Publishing.* [http://dx.doi.org/10.1063/1.4959573]

Spin current, the motion of spin angular momentum, has attracted intense interest due to the prospects of low-energy-consumption spintronic devices.[1,2] Several experimental techniques have been developed to generate and manipulate the spin current, e.g., spin pumping,[3–5] spin Seebeck effect,[6–8] and spin-Hall effect (SHE).[9–11] Recently, the generation and propagation of spin current in antiferromagnets (AFMs) have been extensively investigated by various techniques.[12–22] Especially, the thermally injected or dynamically pumped spin current from ferromagnetic (FM) $Y_3Fe_5O_{12}$ (YIG) layer can flow into the NiO or CoO antiferromagnetic insulator (AFMI) layer and reach the Pt or Ta nonmagnetic metal (NM) layer where it can be converted into charge current by means of the inverse spin-Hall effect (ISHE).[18–22] By introducing a thin AFMI layer, the ISHE voltage is largely enhanced and exhibits a nonmonotonic temperature or an AFMI thickness dependence, with a maximum value appearing near the anti-ferromagnetic (AFM) ordering temperature of AFMI or at the AFMI thickness of ∼1–2 nm, respectively.[18–22]

Several theoretical models have been proposed for the propagation of injected spin current through AFMs in NM/AFM/FM heterostructures.[23–26] These models describe the spin-current transport and its enhancement by assuming that the AFMs are ordered at room temperatures, while the ordering temperatures of thin AFM films are well below the room temperature.[27] In most of these experimental or theoretical

investigations, the spin current carried by spin waves is produced in YIG layer and flows into the AFMI layer.[18–26] In this paper, we provide an alternative method of spin current source, namely, the spin current is generated in the Pt layer via SHE[9–11] and the YIG layer serves merely as a spin current absorber. Specifically, we study the magnetoresistance in Pt/NiO/YIG heterostructures in which the spin-Hall magnetoresistance (SMR) has been correlated with the spin current absorbed by the YIG layer.

The Pt/NiO/YIG heterostructures were prepared on (111)-orientated $Gd_3Ga_5O_{12}$ (GGG) substrates in a combined ultra-high vacuum (10^{-9} Torr) pulse laser deposition (PLD) and sputter system. The high-quality YIG and NiO layers were deposited via PLD technique. The deposition temperature and oxygen pressure were kept at 750 °C and 80 mTorr for YIG growth, and at 600 °C and 50 mTorr for NiO growth, respectively. The energy density and the frequency of laser are 4 J/cm^2 and 2 Hz, respectively. The distance between target and substrate is around 55 mm. After growth, the samples were annealed under the depositing conditions for 1 h to ensure a complete and homogeneous oxygenation. The top Pt films were sputtered in an *in situ* process in a 4 mTorr argon atmosphere at room temperature. In this study, the thicknesses of YIG and Pt layers are fixed at 60 and 3 nm, respectively, while the NiO thickness ranges from 0 to 8 nm. Figure 1(a) plots a representative x-ray diffraction (XRD) pattern for an epitaxial YIG film near the (444) reflection. Clear Laue oscillations indicate an ideal flatness and uniformity of the prepared film. As shown in Fig. 1(b), no indication of impurities or misorientation was detected in the range of 20°–80°. The atomic force microscopy surface topography of Pt/NiO(3)/YIG heterostructure over an area of 3 μm × 3 μm in Fig. 1(c)

---

a)Present address: Swiss Light Source and Laboratory for Scientific Developments and Novel Materials, Paul Scherrer Institute, CH-5232 Villigen PSI, Switzerland
b)Electronic mail: zhanqf@nimte.ac.cn
c)Electronic mail: zhangshu@email.arizona.edu
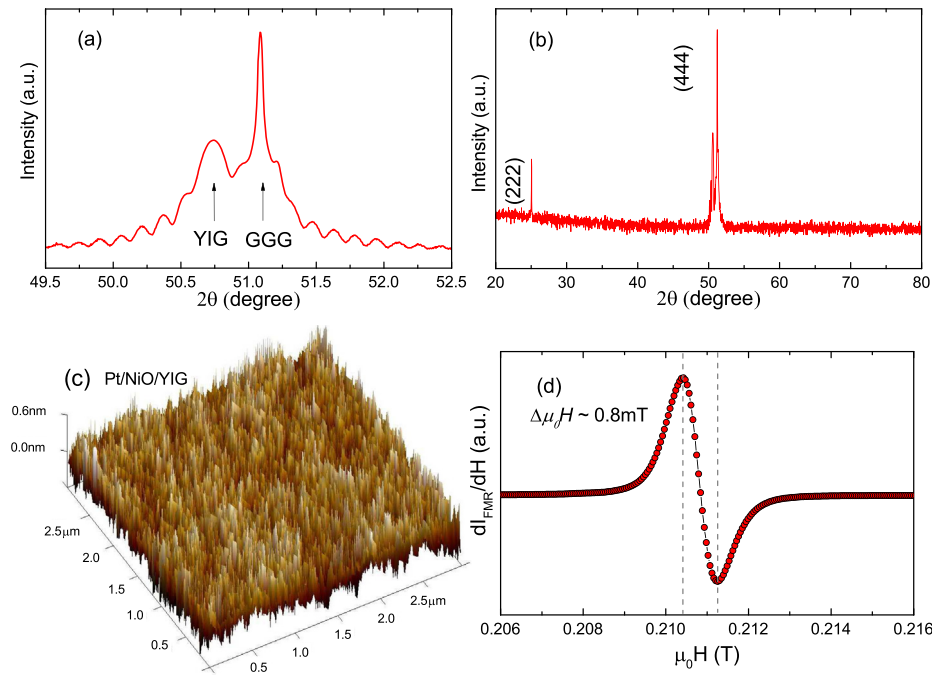d)Electronic mail: runweili@nimte.ac.cn

FIG. 1. The representative 2θ-ω XRD patterns for a YIG/GGG film (a) near the (444) reflections and (b) from 20° to 80°. (c) Three dimensional plot of the atomic force microscope surface topography for Pt/NiO(3)/YIG over an area of $3\,\mu m \times 3\,\mu m$. (d) A representative FMR derivative absorption spectrum of YIG film.

reveals a root-mean-square surface roughness of 0.14 nm (the number in the brackets shows the thickness of NiO layer in nm), indicating that the prepared films are atomically flat. A representative ferromagnetic resonance (FMR) derivative absorption spectrum of YIG films shown in Fig. 1(d) exhibits a peak-to-peak value $\Delta\mu_0 H$ of 0.8 mT, which was measured at a radio frequency of 9.39 GHz and a power of 0.1 mW with an in-plane magnetic field at room temperature. The estimated damping constant $\alpha = 2.1 \times 10^{-3}$ is comparable with the previously reported value.[28] For a reference, Pt/NiO/MgO(001) heterostructures were additionally prepared by using the above parameters.

As shown in the right panel of Fig. 2, all the films were patterned into a Hall-bar geometry (central area: 0.3 mm × 10 mm; electrodes: 0.3 mm × 1 mm) by using a shadow mask during the growth. The anisotropic magnetoresistance (AMR) were measured in a magnetic field of 2 T for both

Pt/NiO/YIG and Pt/NiO/MgO heterostructures. The absence of AMR in Pt/NiO/MgO implies that the NiO moments cannot be polarized by such magnetic field. Both the Pt/YIG and Pt/NiO(1)/YIG heterostructures demonstrate a clear SMR with the amplitudes reaching 6.1×10^{-4} and 4.5×10^{-4} at room temperature, respectively [see Figs. 2(c) and 2(f)], implying that the spin current generated by SHE in Pt can transport through NiO and interact with YIG. Apparently, the spin current can pass through NiO from both directions, i.e., Pt → NiO → YIG or YIG → NiO → Pt.[18,19,22] For Pt/YIG, as shown in Fig. 2(b), a conventional AMR (CAMR) induced by the magnetic proximity effect (MPE) always coexists with the SMR and its maximum amplitude of 2.2×10^{-4} is comparable to the SMR. However, for Pt/NiO(1)/YIG, there is no clear CAMR at any temperatures [see Fig. 2(e)], and the observed AMR in xy plane (θ_{xy}) is entirely from the SMR. As shown in Figs. 2(d) and 2(f), the
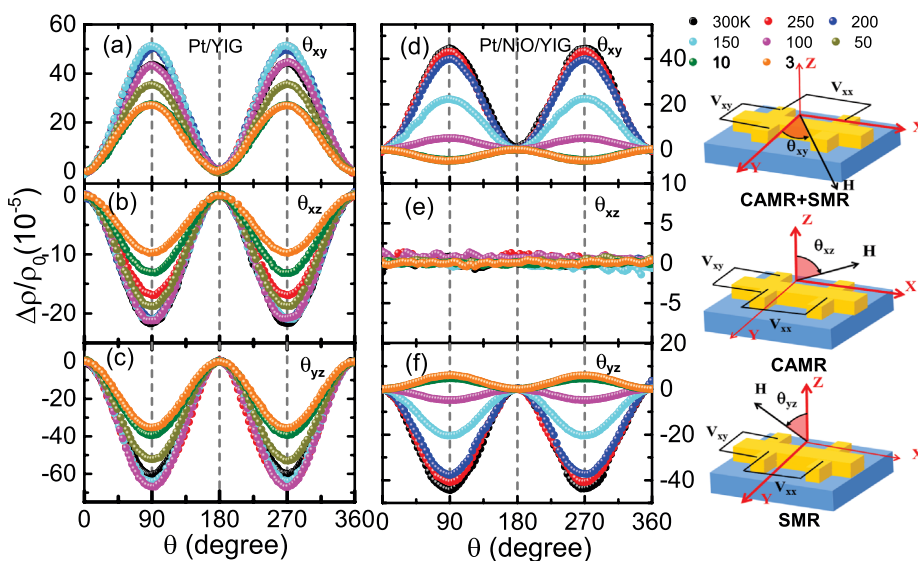

FIG. 2. The AMR at various temperatures for (a)–(c) Pt/YIG and (d)–(f) Pt/NiO(1)/YIG with magnetic field varied within the xy, xz, and yz planes. The right panel shows the schematic plots of the longitudinal and transverse resistance measurements. The magnetic field orientations θ_{xy}, θ_{xz}, and θ_{yz} are with respect to the y-, z-, and z-axes, respectively. The electric current is applied along the x-axis.
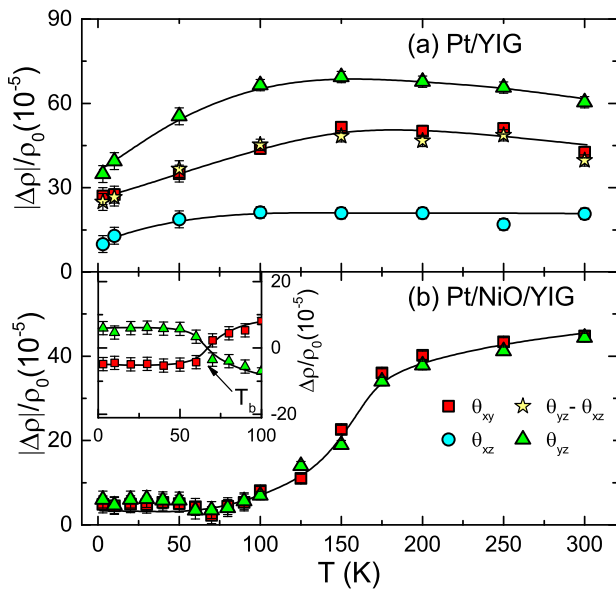
FIG. 3. Temperature dependence of AMR amplitude for (a) Pt/YIG and (b) Pt/NiO(1)/YIG heterostructures. The cubic, circle, and triangle symbols stand for the θ_{xy}, θ_{xz}, and θ_{yz} scans, respectively. The stars represent the difference between the SMR and the CAMR ($\theta_{yz} - \theta_{xz}$). The inset of (b) shows the $\Delta\rho/\rho_0$ below 100 K for Pt/NiO(1)/YIG. The solid lines are guides to the eye.

θ_{xy} and θ_{yz} scans exhibit a similar behavior, reinforce the notion that the MPE on Pt is completely destroyed by the NiO layer. Further support on the absence of MPE is provided by the anomalous Hall resistance (AHR). For instance, the AHR at 7 T for Pt/NiO(1)/YIG is 4.6 mΩ at 5 K, which is 6 times smaller than the value of 27.6 mΩ for Pt/YIG. For $t_{NiO} \geq 3$ nm, the AHR becomes undetectable. Compared to the Pt/IrMn/YIG, Pt/Cu/YIG, or Pt/Au/YIG heterostructures, only 26% of the SMR is lost by the insertion of 1 nm NiO layer, while over 80% of the SMR is suppressed by the insertion of 1 nm IrMn, Cu, or Au layer at room temperature.[29–31] Our experiments illustrate that the NiO inserted layer could efficiently block the MPE while still allow the transport of most of the spin current at room temperature.

All the AMR amplitudes are summarized in Fig. 3 as a function of temperature. For Pt/YIG, the SMR exhibits a nonmonotonic temperature dependence and acquires its maximum value of 6.9×10^{-4} around 150 K. While for θ_{xy} scan

in which both CAMR and SMR contribute to the total AMR, the amplitude is almost identical to the difference between SMR and CAMR [see stars in Fig. 3(a)], i.e., $|\Delta\rho|/\rho_0(\theta_{xy}) = |\Delta\rho|/\rho_0(\theta_{yz}) - |\Delta\rho|/\rho_0(\theta_{xz})$. After inserting a NiO layer, as shown in Fig. 3(b), $|\Delta\rho|/\rho_0(\theta_{xy}) = |\Delta\rho|/\rho_0(\theta_{yz})$, which indicates that the SMR dominates the AMR for θ_{xy} scan due to the absence of MPE. Similar results have been previously reported in MPE-free Rh/YIG bilayers.[32]

The temperature dependence of the SMR is highly nontrivial. The magnitude of the SMR decreases sharply when the temperature becomes lower than the blocking temperature. Qualitatively, one may attribute the decrease to the reduction of the number of AFM magnons[22] since the spin current carriers in the NiO layer magnons whose population rapidly decreases as temperature decreases. What is more interesting is the SMR changes sign around 70 K, and then the SMR stays at a constant value below 70 K, about 10 times smaller than that of room temperature. The magnetic characterization for the exchange bias field suggests that the NiO moments in Pt/NiO(1)/YIG become antiferromagnetcially ordered when approaching the blocking temperature $T_b \sim 70$ K (see details in Fig. 4). At present, it is unclear what governs the low temperature SMR behavior; it appears to be correlated with the formation of the AFM ordering.

The AFM ordering temperature for a very thin AFM film is expected to be well below the corresponding Néel temperature.[27] It is rather difficult to measure the ordering temperature on the ultrathin AFM film. One approximate way is to study temperature dependence of exchange bias field H_e in which the blocking temperature is defined as the H_e reduces to zero. However, the ordering temperature could be quite different from the blocking temperature since the former characterizes the long range exchange correlation while the latter is simple description of the AFM anisotropy constant. Nevertheless, we present the exchange bias data to approximately estimate the ordering temperature. Figure 4(a) shows the typical hysteresis loops at various temperatures for Pt/NiO(1)/YIG. The blocking temperatures are approximately determined to be around 70, 110, and 150 K for the Pt/NiO/YIG heterostructures with 1, 3, and 5 nm NiO inserted layers, respectively. The coercivity H_c exhibits a sudden increase near T_b, as shown in the inset of Fig. 4(b).
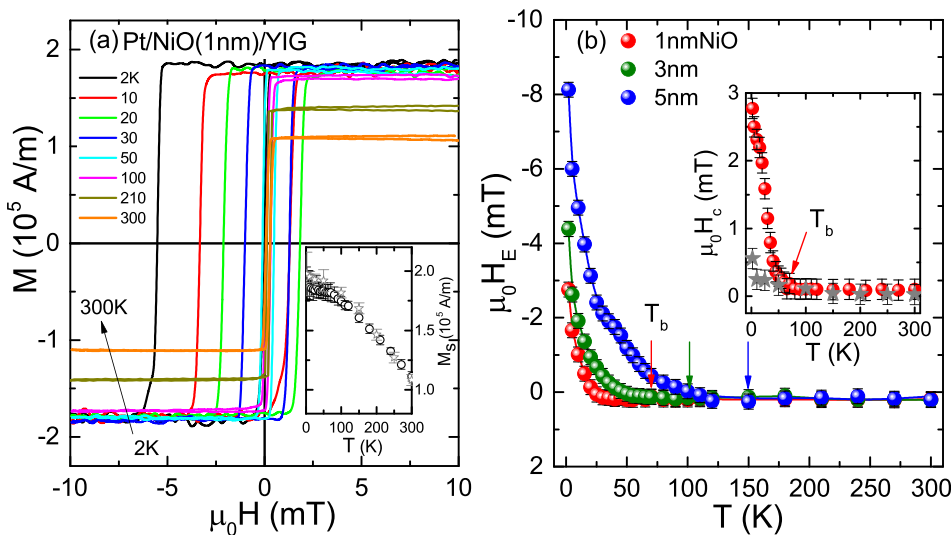

FIG. 4. (a) Hysteresis loops for Pt/NiO(1)/YIG at various temperatures. The inset shows the saturation magnetization M_s versus temperature for Pt/YIG (stars) and Pt/NiO(1)/YIG (circles). (b) Temperature dependent H_e for Pt/NiO/YIG with different NiO thicknesses. The arrows indicate the blocking temperatures T_b. The inset of (b) plots the temperature dependent coercivity H_c for Pt/YIG (stars) and Pt/NiO(1)/YIG (circles).

While for Pt/YIG films, H_c is rather small for the temperature range from 300 K (<0.1 mT) to 2 K (0.55 mT). The Pt/YIG and Pt/NiO(1)/YIG films have identical temperature dependent saturation magnetization M_s, as shown in the inset of Fig. 4(a), consistent with the previous reported values.[28,33]

We finally comment on the difference on the AFM mediated spin transport between the spin pumping or spin Seebeck result and our SMR result. In the former cases, the spin current was created in the YIG layer and the spin current detected in the Pt was found to be enhanced in the presence of the thin AFMI layer, and furthermore the spin current could penetrate to the AFMI as large as 10 nm.[18–22] In our case, both spin current creation and detection occur in the Pt layer, and we do not find any enhancement compared to the spin current without the AFMI layer, and the SMR disappears when the thickness of the AFMI exceeds 3 nm. On the other hand, there is one common feature: all experiments have shown that the spin current transmission is strongest near or above the ordering temperature of the AFMI. Clearly, magnetic fluctuation is important in all these experiments; however, the different amplitude and thickness dependence of the spin signals in spin pumping or spin Seebeck compared with our data demand further theoretical and experiments on the spin transport physics in AFMIs.

In summary, we investigated the SMR in Pt/NiO/YIG heterostructures over a wide temperature range. The SMR signal is comparable to that without the NiO layer when the temperature is near or above the blocking temperature of the NiO, but significantly suppressed at low temperatures. On the other hand, the CAMR is practically zero, implying that the insertion of the NiO has completely destroyed the Pt magnetization induced by the YIG MPE. The dual roles of the thin NiO layer are to suppress the magnetic interaction or MPE between Pt and YIG, and to maintain efficient spin current transmission at high temperature.

[1]S. Maekwa, *Spin Current* (Oxford University Press, Oxford, 2012).
[2]M. Z. Wu and A. Hoffmann, *Recent Advances in Magnetic Insulators—From Spintronics to Microwave Applications* (Academic Press, San Diego, 2013), Vol. 64.
[3]B. Heinrich, C. Burrowes, E. Montoya, B. Kardasz, E. Girt, Young-Yeal Song, Y. Sun, and M. Z. Wu, Phys. Rev. Lett. **107**, 066604 (2011).
[4]S. M. Rezende, R. L. Rodríguez-Suárez, M. M. Soares, L. H. Vilela-Leao, D. Ley Domínguez, and A. Azevedo, Appl. Phys. Lett. **102**, 012402 (2013).
[5]Y. Kajiwara, K. Harii, S. Takahashi, J. Ohe, K. Uchida, M. Mizuguchi, H. Umezawa, H. Kawai, K. Ando, K. Takanashi, S. Maekawa, and E. Saitoh, Nature **464**, 262 (2010).
[6]K. Uchida, S. Takahashi, K. Harii, J. Ieda, W. Koshibae, K. Ando, S. Maekawa, and E. Saitoh, Nature **455**, 778 (2008).
[7]K. Uchida, J. Xiao, H. Adachi, J. Ohe, S. Takahashi, J. Ieda, T. Ota, Y. Kajiwara, H. Umezawa, H. Kawai, G. E. W. Bauer, S. Maekawa, and E. Saitoh, Nat. Mater. **9**, 894 (2010).
[8]G. E. W. Bauer, E. Saitoh, and B. J. van Wees, Nat. Mater. **11**, 391 (2012).
[9]J. E. Hirsch, Phys. Rev. Lett. **83**, 1834 (1999).
[10]J. Wunderlich, B. Kaestner, J. Sinova, and T. Jungwirth, Phys. Rev. Lett. **94**, 047204 (2005).
[11]Y. K. Kato, R. C. Myers, A. C. Gossard, and D. D. Awschalom, Science **306**, 1910 (2004).
[12]J. B. S. Mendes, R. O. Cunha, O. Alves Santos, P. R. T. Ribeiro, F. L. A. Machado, R. L. Rodríguez-Suárez, A. Azevedo, and S. M. Rezende, Phys. Rev B **89**, 140406(R) (2014).
[13]W. Zhang, M. B. Jungfleisch, W. Jiang, J. E. Pearson, A. Hoffmann, F. Freimuth, and Y. Mokrousov, Phys. Rev. Lett. **113**, 196602 (2014).
[14]L. Frangou, S. Oyarzún, S. Auffret, L. Vila, S. Gambarelli, and V. Baltz, Phys. Rev. Lett. **116**, 077203 (2016).
[15]J. Sinova, S. O. Valenzuela, J. Wunderlich, C. H. Back, and T. Jungwirth, Rev. Mod. Phys. **87**, 1213 (2015) and reference therein.
[16]X. Zhou, L. Ma, Z. Shi, W. J. Fan, J. G. Zheng, R. F. L. Evans, and S. M. Zhou, Phys. Rev. B **92**, 060402(R) (2015).
[17]S. Seki, T. Ideue, M. Kubota, Y. Kozuka, R. Takagi, M. Nakamura, Y. Kaneko, M. Kawasaki, and Y. Tokura, Phys. Rev. Lett. **115**, 266601 (2015).
[18]C. Hahn, G. de Loubens, O. Klein, M. Viret, V. V. Naletov, and J. B. Youssef, Europhys. Lett. **108**, 57005 (2014).
[19]H. L. Wang, C. H. Du, P. C. Hammel, and F. Y. Yang, Phys. Rev. Lett. **113**, 097202 (2014).
[20]H. L. Wang, C. H. Du, P. C. Hammel, and F. Y. Yang, Phys. Rev. B **91**, 220410(R) (2015).
[21]Z. Qiu, J. Li, D. Hou, E. Arenholz, A. T. NDiaye, A. Tan, K. Uchida, K. Sato, Y. Tserkovnyak, Z. Q. Qiu, and E. Saitoh, e-print arXiv:1505.03926.
[22]W. Lin, K. Chen, S. Zhang, and C. L. Chien, Phys. Rev. Lett. **116**, 186601 (2016).
[23]R. Cheng, J. Xiao, Q. Niu, and A. Brataas, Phys. Rev. Lett. **113**, 057601 (2014).
[24]S. Takei, T. Moriyama, T. Ono, and Y. Tserkovnyak, Phys. Rev. B **92**, 020409(R) (2015).
[25]R. Khymyn, I. Lisenkov, V. S. Tiberkevich, A. N. Slavin, and B. A. Ivanov, Phys. Rev. B **93**, 224421 (2016).
[26]S. M. Rezende, R. L. Rodríguez-Suárez, and A. Azevedo, Phys. Rev. B **93**, 014425 (2016).
[27]A. Baruth and S. Adenwalla, Phys. Rev. B **78**, 174407 (2008).
[28]M. C. Onbasli, A. Kehlberger, D. H. Kim, G. Jakob, M. Kläui, A. V. Chumak, B. Hillebrands, and C. A. Ross, APL Mater. **2**, 106102 (2014) and reference therein.
[29]Y. T. Chen, S. Takahashi, H. Nakayama, M. Althammer, S. T. B. Goennenwein, E. Saitoh, and G. E. W. Bauer, J. Phys. Condens. Matter **28**, 103004 (2016) and reference therein.
[30]T. Shang, H. L. Yang, Q. F. Zhan, Z. H. Zuo, Y. L. Xie, L. P. Liu, S. L. Zhang, Y. Zhang, H. H. Li, B. M. Wang, Y. H. Wu, S. Zhang, and R.-W. Li, e-print arXiv:1603.03578.
[31]M. Althammer, S. Meyer, H. Nakayama, M. Schreier, S. Altmannshofer, M. Weiler, H. Huebl, S. Geprägs, M. Opel, R. Gross, D. Meier, C. Klewe, T. Kuschel, J. M. Schmalhorst, G. Reiss, L. M. Shen, A. Gupta, Y. T. Chen, G. E. W. Bauer, E. Saitoh, and S. T. B. Goennenwein, Phys. Rev. B **87**, 224401 (2013).
[32]T. Shang, Q. F. Zhan, H. L. Yang, Z. H. Zuo, Y. L. Xie, H. H. Li, L. P. Liu, B. M. Wang, Y. H. Wu, S. Zhang, and R.-W. Li, Sci. Rep. **5**, 17734 (2015).
[33]P. Jang, S. Yamamoto, and H. Kuniki, Phys. Status Solidi (a) **201**, 1851 (2004).